The EMBO Journal (2006) 25, 834–845 | © 2006 European Molecular Biology Organization | All Rights Reserved 0261-4189/06
www.embojournal.org

THE EMBO JOURNAL

Mammalian Emi2 mediates cytostatic arrest and transduces the signal for meiotic exit via Cdc20

Shisako Shoji, Naoko Yoshida, Manami Amanai, Maki Ohgishi, Tomoyuki Fukui, Satoko Fujimoto, Yoshikazu Nakano, Eriko Kajikawa and Anthony CF Perry*

Laboratory of Mammalian Molecular Embryology, RIKEN Center for Developmental Biology, Chuo-ku, Kobe, Japan

Fertilizable mammalian oocytes are arrested at the second meiotic metaphase (mII) by the cyclinB-Cdc2 heterodimer, maturation promoting factor (MPF). MPF is stabilized via the activity of an unidentified cytostatic factor (CSF), thereby suspending meiotic progression until fertilization. We here present evidence that a conserved 71 kDa mammalian orthologue of *Xenopus* XErp1/Emi2, which we term endogenous meiotic inhibitor 2 (Emi2) is an essential CSF component. Depletion *in situ* of Emi2 by RNA interference elicited precocious meiotic exit in maturing mouse oocytes. Reduction of Emi2 released mature mII oocytes from cytostatic arrest, frequently inducing cytodegeneration. Mos levels autonomously declined to undetectable levels in mII oocytes. Recombinant Emi2 reduced the propensity of mII oocytes to exit meiosis in response to activating stimuli. Emi2 and Cdc20 proteins mutually interact and Cdc20 ablation negated the ability of Emi2 removal to induce metaphase release. Consistent with this, Cdc20 removal prevented parthenogenetic or sperm-induced meiotic exit. These studies show in intact oocytes that the interaction of Emi2 with Cdc20 links activating stimuli to meiotic resumption at fertilization and during parthenogenesis in mammals.

The EMBO Journal (2006) **25,** 834–845. doi:10.1038/sj.emboj.7600953; Published online 2 February 2006
Subject Categories: cell cycle; development
Keywords: cytostatic factor; fertilization; metaphase II oocyte; RNAi; XErp1/Emi2

Introduction

Abortive initiation of development in the absence of a paternal genome is prevented in mammalian oocytes by maturation promoting factor (MPF), which sustains metaphase II (mII). MPF activity is in turn maintained by cytostatic factor (CSF) until its abrogation by sperm-induced signaling at fertilization causes meiotic exit (Masui and Markert, 1971; Masui, 2000; Runft *et al*, 2002).

*Corresponding author. Laboratory of Mammalian Molecular Embryology, RIKEN Center for Developmental Biology, 2-2-3 Minatojima Minamimachi, Chuo-ku, Kobe 650-0047, Japan.
Tel.: +81 78 306 3054; Fax: +81 78 306 3144;
E-mail: tony@cdb.riken.jp

Received: 29 August 2005; accepted: 8 December 2005; published online: 2 February 2006

In *Rana pipiens*, ooplasmic CSF activity induces cytostatic arrest when injected into 2-cell blastomeres (Masui and Markert, 1971). Consistent with roles for them in CSF arrest, injection of cRNA encoding Mos, Rsk, or constitutively active MAPK induces cytostasis in *Xenopus* 2-cell embryos (Sagata *et al*, 1989; Haccard *et al*, 1993; Gross *et al*, 1999) and oocytes from gene targeted mice lacking the Mos ortholog, $p42^{mos}$, often undergo parthenogenetic activation (Colledge *et al*, 1994; Hashimoto *et al*, 1994). However, not all do (Hashimoto *et al*, 1994) and Ca^{2+}-induced MPF destruction precedes Mos inactivation in *Xenopus* (Watanabe *et al*, 1991). Moreover, MPF kinase activity in Mos-deficient mouse oocytes is normal until late mII (Choi *et al*, 1996).

In mitosis, the activity of MPF is regulated by the anaphase promoting complex/cyclosome (APC), a multimeric E3 ubiquitin ligase with similarities to other ubiquitin ligases including SCF (Skp1, Cullin and F-box protein) (Murray *et al*, 1989; Yu *et al*, 1998). The APC modulates MPF activity via the destruction of cyclin B (Murray *et al*, 1989) and becomes active when bound by Cdc20 or Cdh1 proteins (Page and Hieter, 1999).

Because of its central mitotic role in regulating MPF, attention has focused on the APC in meiosis. In *Xenopus* oocyte extracts and mitotic cells, the spindle assembly checkpoint (SAC) proteins, Mad1, Mad2 and BubR1, are able to inhibit the APC by sequestering Cdc20 (Li *et al*, 1997; Fang *et al*, 1998; Tang *et al*, 2001) and the establishment and/or maintenance of CSF-mediated mII arrest requires Mad1, Mad2 and Bub1 (Tunquist *et al*, 2002, 2003). This situation contrasts with mice, in which the SAC is not essential for CSF arrest as evidenced by experiments in which disruption of Bub1, Mad2 or BubR1 function does not prevent it (Tsurumi *et al*, 2004).

The APC is also reportedly regulated in *Xenopus* oocyte extracts via the binding of Cdc20 by the early mitotic inhibitor, Emi1 (Reimann *et al*, 2001). Extracts immunodepleted of Emi1 degraded cyclin B and exited from meiotic arrest prematurely, an effect that could be blocked by the addition of a recombinant C-terminal Emi1 fusion protein (Reimann and Jackson, 2002). However, Emi1 is reduced to subfunctional levels in *Xenopus* prometaphase, contradicting a contribution to metaphase arrest (Ohsumi *et al*, 2004) and its relationship to CSF-mediated mII arrest remains unclear (Tung *et al*, 2005).

Arrest at mII is resolved by an oocyte activating signal physiologically delivered by a spermatozoon (Runft *et al*, 2002). Activation involves the mobilization of intracellular free calcium, Ca_i^{2+}; fertilization generates a series of Ca_i^{2+} oscillations (Kline and Kline, 1992; Runft *et al*, 2002). It has recently been shown that a component of the sperm-borne oocyte activating factor (SOAF) that triggers Ca_i^{2+} oscillations is phospholipase Cζ (Saunders *et al*, 2002; Fujimoto *et al*, 2004). Parthenogenetic activation by Sr^{2+} and sperm-induced activation potentiate full development at significantly different rates (Perry *et al*, 1999) and it is not

known whether sperm-induced oocyte activation and parthenogenesis occur via the same pathway.

We sought to probe the relationship between SOAF and meiotic resumption by investigating the molecular nature of CSF in the mouse. A database search identified a CSF candidate, which we designated endogenous meiotic inhibitor 2, Emi2. We show in intact mouse oocytes that Emi2 is required to establish and maintain metaphase arrest and that this faculty is dependent upon the presence of Cdc20 protein.

Results

Oocyte activation is accompanied by reduction in levels of the conserved F-box protein, Emi2

Database searching identified a mouse Emi1-like sequence, designated endogenous meiotic inhibitor 2, Emi2 (Genbank BC 098484). Mouse Emi1 and Emi2 predicted proteins share 21% sequence identity and a similar arrangement of βTrCP, F-box and Zn-binding domains (Figure 1A). Emi2 is evolutionarily conserved (Figure 1B) and while this work was in train, its *Xenopus* ortholog, XErp1/Emi2, was reported to exhibit cytostatic activity (Schmidt *et al*, 2005; Tung *et al*, 2005). RT–PCR of mouse (Figure 1C) and *Xenopus* (data not shown) tissues suggested widespread Emi1 expression, whereas Emi2 was restricted to testis and ovary (Figure 1C). In the mouse, Emi1 mRNA was detected in immature and mII oocytes and throughout preimplantation development, but Emi2 mRNA, which was detectable in immature and mII oocytes, diminished after oocyte activation (Figure 1D).

Immunoblots probed with Emi1-non-reactive, anti-Emi2 antibodies (Figure 1E) identified a protein of 71 kDa, whose

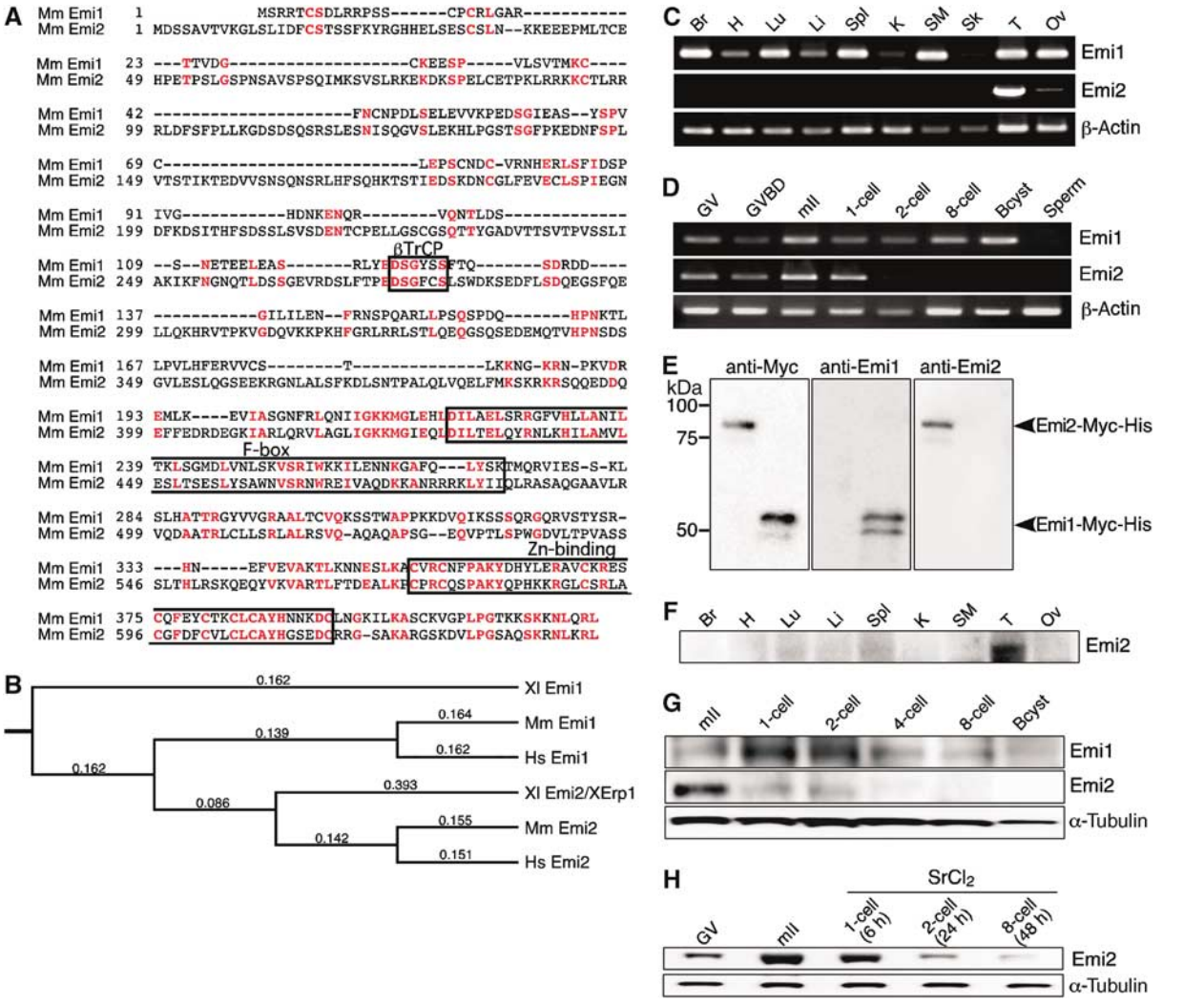

Figure 1 Emi2 expression is tissue specific and declines after oocyte activation, and its relationship to Emi1. (**A**) Alignment of mouse Emi1 and Emi2 predicted amino-acid sequences showing conserved domains. Identities are indicated in red. Mm, *Mus musculus*. (**B**) Phylogenetic tree of Emi1 and Emi2 orthologs. Numbers indicate bootstrap support from neighbour jointing. Xl, *Xenopus laevis*; Mm, *Mus musculus*; Hs, *Homo sapiens*. RT–PCR for mouse Emi1, Emi2 and β-actin transcripts in different tissues (**C**) and in gametes and preimplantation embryonic development (**D**), showing 0.75–3.3 cell equivalents per lane. β-Actin served as an internal control. GV, germinal vesicle; GVBD, GV breakdown. (**E**) Immunoblotting of recombinant Emi2-Myc-His (left in each panel) and Emi1-Myc-His to show mutual specificity of anti-Emi1 and -Emi2 polyclonal antibodies. (**F**) Tissue immunoblotting showing levels of Emi2 protein in brain (Br), heart (H), lung (Lu), liver (Li), spleen (Spl), kidney (K), skeletal muscle (SM), testis (T) and ovary (Ov); 30 μg total protein were loaded per lane. Immunoblotting showing levels of Emi1 and Emi2 in oocytes and at different preimplantation developmental stages derived by (**G**) natural mating, or (**H**) of Emi2 in a developmental time course for $SrCl_2$-induced parthenogenotes. The gels of (G) and (H) were, respectively, loaded with 30 or 60 oocytes or embryos per lane.

expression in different tissues mirrored that of its mRNA (Figure 1F). Expression was particularly pronounced in the testis. Emi2 protein was present in mII oocytes (Figure 1G), although its level declined following activation either by sperm (fertilization) or $SrCl_2$-induced parthenogenesis and in either case became undetectable around the 8-cell stage (Figure 1G and H).

Contrastingly, anti-Emi1 antibodies identified a weakly reactive protein of 48 kDa in mII oocytes (Figure 1G). Unlike Emi2, Emi1 persisted throughout preimplantation development and was detected at levels 1.2- to 1.5-fold higher than those of mII oocytes in the first two cell cycles (Figure 1G).

These findings are consistent with a role for Emi2 in CSF arrest. We therefore sought to determine whether Emi2 contributed to CSF activity in intact mouse oocytes.

Negligible induction of cytostatic arrest by microinjecting mouse embryos with native CSF

Cytostatic activity was first demonstrated in the frog, *Rana pipiens*; injecting a 2-cell blastomere with 10–12% of its volume of mature mII cytoplasm caused cell cycle arrest in 70–86% of cases (Masui and Markert, 1971). Contrastingly, in the mouse, fusion of entire mII oocytes with fertilization-produced 2-cell blastomeres failed to induce cytostatic arrest, although some cytostatic activity could be demonstrated when fusion was with the 2-cell blastomeres of parthenogenotes (Zernicka-Goetz *et al*, 1995). There are no reports of mammalian cytostatic activity having been elicited by microinjection of 2-cell blastomeres with mII ooplasm, although this is an essential control for the demonstration of Emi2-mediated CSF activity by microinjection.

To pursue this in mouse oocytes, we injected 15 to >25pl mII (17–22 h post-hCG) cytoplasm into 1-cell (5–6 h postactivation) or 2-cell (24 h post-activation) parthenogenetic embryos; 25 pl is ~18% of the volume of a 2-cell mouse blastomere. However, mII cytoplasmic transfer exerted only a marginal effect, if any, on embryo cleavge (Figure 2A).

To control against postinjection leakage (Masui and Markert, 1971) and verify stable mII cytoplasmic transfer, we injected donor cytoplasm from transgenic mII oocytes expressing a mitochondrially targeted GFP spectral variant, Venus (Figure 2B) (Okita *et al*, 2004). Injected 2-cell embryos failed to undergo significant cytostatic arrest 24 h postinjection relative to controls (Figure 2A and C). Venus protein was detected in the injected blastomere of 2-cell embryos soon (2 h) after injection (Figure 2B). Venus was present 24 h after injection in two blastomeres of 4-cell embryos following cleavage (Figure 2C). Since mouse mitochondrial replication does not initiate prior to the blastocyst stage (Pikó and Taylor,

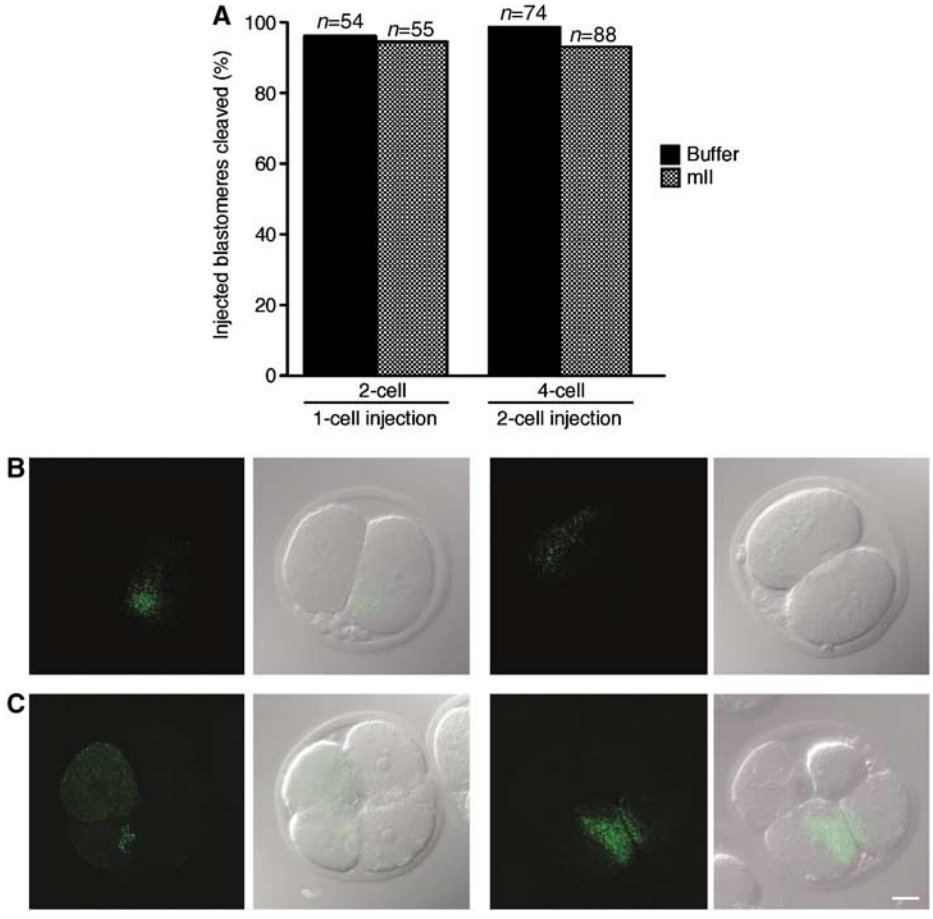

Figure 2 Injection of mouse mII ooplasm into 1- or 2-cell mouse embryos does not elicit cytostatic arrest. (**A**) Percentages of embryos whose blastomeres had undergone cell division 24 h after injection with buffer (filled) or mII ooplasm (stippled). Paired images show epifluorescence (left) merged with DIC (right) microscopy of embryos (**B**) 2 h or (**C**) 24 h after injection of 2-cell blastomeres with cytoplasm from mII oocytes transgenic for mitochondrially localized Venus protein. Bar = 20 μm.

1987), these data confirm that transfer of a significant volume of mII cytoplasm had occurred without leakage. Thus, and in contrast to the situation in *R. pipiens* and *Xenopus*, CSF activity cannot necessarily be demonstrated in the mouse by microinjecting mII cytoplasm into 1- or 2-cell embryos.

Emi2 promotes metaphase arrest in maturing germinal vesicle oocytes

We therefore adopted an alternative strategy based on RNA interference (RNAi) to probe candidate cytostatic activities (Svoboda *et al*, 2000; Wianny and Zernicka-Goetz, 2000; Kim *et al*, 2002). We harnessed the pronounced specificity of carefully designed short interfering RNAs (siRNAs) (Haley and Zamore, 2004).

The efficacy of two sequence-specific siRNAs (siEmi1#2 and siEmi1#3) mapping to nonoverlapping regions of Emi1 mRNA was shown in surrogate assays (Huppi *et al*, 2005). siEmi1#2 or siEmi1#3 were co-transfected with an Emi1-EGFP or -Myc fusion construct into NIH3T3 or HEK293T cells. Fluorescence and Emi1 mRNA and protein levels were depleted compared to controls (Supplementary Figure S1A–C).

This paved the way for an evaluation of Emi1 during oocyte maturation. Injection of germinal vesicle (GV) oocytes with Emi1 siRNAs reduced the level of Emi1 mRNA by an average of 91.5% ($n=4$) after 28–30 h (Figure 3A; Supplementary Figure S2A). However, in common with *in vitro* matured (IVM) control oocytes, maturing oocytes injected with Emi1 siRNA arrested at mII (Figure 3B–D) as judged by their morphology and relatively high levels of MBP and H1 phosphorylation, respectively, reflecting high MAPK and MPF kinase activities (Figure 3E). This arrest persisted 50 h after siRNA injection.

We next investigated whether instead, Emi2 mRNA depletion might affect meiotic arrest. Two nonoverlapping Emi2 siRNAs (siEmi2#1 and siEmi2#2) eliminated recombinant Emi2 mRNA and protein expression in the surrogate assay (Supplementary Figure S1D and E). As expected, Emi2 siRNAs did not demonstrably effect recombinant Emi1 protein expression in transfected cells (data not shown) or Emi1 transcript levels in oocytes, and *vice versa* (Figure 3A and below). When injected into GV oocytes, Emi2 siRNAs caused a pronounced (97.7%, $n=8$) reduction in Emi2 mRNA (Figure 3A; Supplementary Figure S2A). However, in contrast to the situation with Emi1 or control EGFP siRNAs, GV oocytes injected with either of the Emi2 siRNAs progressed through the cell cycle without arresting at mII (Figure 3B and C and Supplementary movie S1). At 30 h postinjection, most

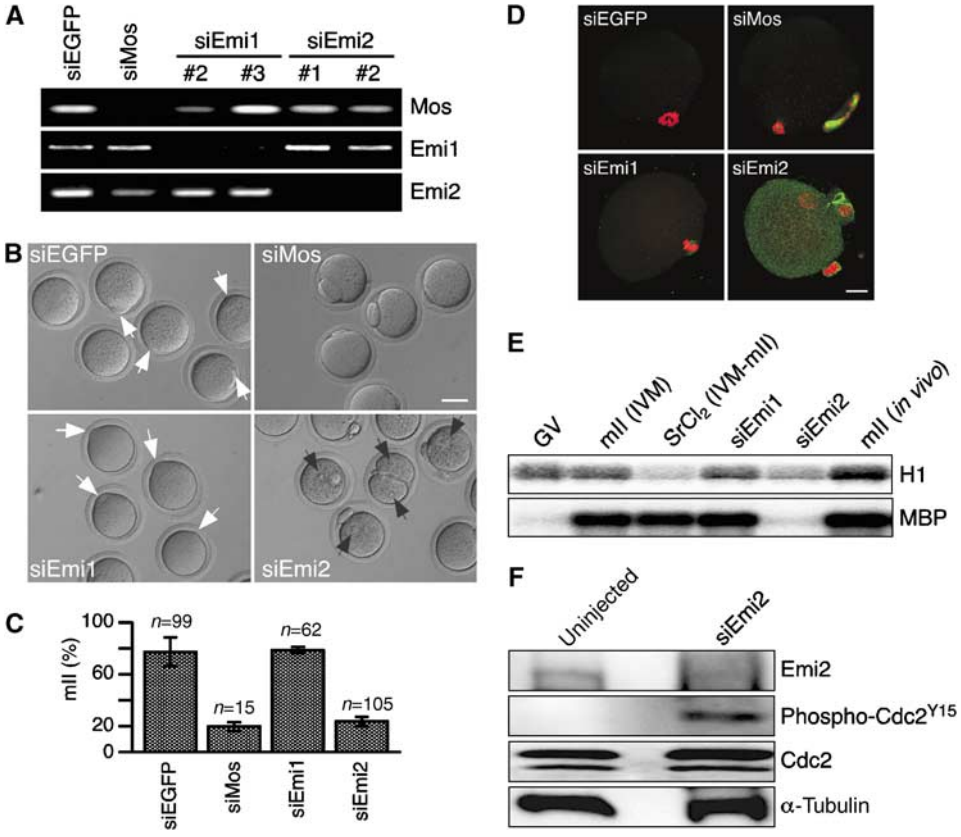

Figure 3 Meiotic progression in maturing mouse oocytes depleted of Emi2 or Mos, but not Emi1 mRNA. (**A**) RT–PCR of Mos, Emi1 and Emi2 transcripts in GV oocytes 29 h after injection with siRNAs for Mos, Emi1 (#2, siEmi1#2; #3, siEmi1#3), Emi2 (#1, siEmi2#1; #2, siEmi2#2) and EGFP. (**B**) Hoffman modulation micrographs of oocytes or embryos 29 h after GV oocyte injection with siEmi1#2, siEGFP, siEmi2#1 and siMos siRNAs. White arrow, mII plate; black arrow, pronucleus. Bar = 50 μm. (**C**) Average percentages of oocytes (showing ranges) with mII morphology 29 h after GV siRNA injection. (**D**) Immunofluorescence microscopy of representative cells in (B) showing α-tubulin (green) and genomic DNA (red). Bar = 20 μm. (**E**) Autoradiograph of myelin basic protein (MBP) and H1 kinase assays, respectively, for MAPK or MPF kinase activities, 29 h after injection of GV oocytes with siEmi1#2 or siEmi2#1. Control GV, *in vitro*-matured (IVM) and *in vivo*-matured mII oocytes are included. (**F**) Western blotting of oocytes 26 h after GV oocyte injection with siEmi2#1, and of age-matched, noninjected controls. In total, 35 oocytes were loaded per lane.

cells had precociously undergone cytokinesis to elaborate one or more polar bodies (Pbs) and contained a structure resembling a pronucleus (Figure 3B–D). Many cells underwent cleavage (see Supplementary movie S1); it is not clear whether this typically reflected an anomalously symmetrical second meiotic cytokinesis or the first mitotic cell division. Depletion of Emi2 mRNA in maturing oocytes caused a marked reduction of MBP and H1 kinase activities (Figure 3E) and was accompanied by a decrease in Emi2 protein and the appearance of (inactive) phospho-Cdc2^{Y15} (Figure 3F). This suggests that Emi2 depletion elicited cell cycle progression in maturing oocytes.

In the same time frame, RNAi following injection of Mos siRNA phenocopied the Mos-deficient oocytes of gene-targeted mice (Figure 3B–D). Maturing Mos *null* oocytes exhibit retarded cell cycle progression relative to their wild-type counterparts (Hashimoto *et al*, 1994; Choi *et al*, 1996). The absence of pronuclei in siMos-injected oocytes 29 h post-injection (Figure 3B), and the presence of relatively condensed chromatin (Figure 3D) suggested similar cell cycle retardation, with fluorescence micrographs resembling those previously presented for *mos*$^{-/-}$ oocytes (Choi *et al*, 1996). Moreover, the Pb_1 of *mos*$^{-/-}$ maturing oocytes persists instead of degrading, as it does typically within 7 h of extrusion in wild-type oocytes (Choi *et al*, 1996). We found that maturing oocytes injected with siMos were also associated with pronounced Pb_1s 29 h later, with no signs of Pb degeneration (Figure 3B). Finally, failure of the spindle to translocate to the cortex in maturing *mos*$^{-/-}$ oocytes generates an anomalously large Pb_1 (Choi *et al*, 1996). Enlarged Pb_1s are also clearly discernable following siMos-induced RNAi (Figure 3B) and have been reported elsewhere for maturing oocytes injected with Mos siRNA (Kim *et al*, 2002).

Emi2 is required to maintain mammalian mII arrest

Whereas CSF activity is required to maintain mII arrest (Masui, 2000), it is not necessarily required to establish it. To discriminate between roles in mII establishment and maintenance, we therefore injected mature mII oocytes with either Emi1, Emi2 or Mos siRNA. Following incubation for 20–31 h, Emi1 and Emi2 target mRNA levels declined at least 97.3% ($n \geqslant 22$) compared to controls (Figure 4A and Supplementary Figure S2B; Mos is discussed below). mII oocytes injected with Emi1, Mos or control EGFP siRNAs remained at metaphase (Figure 4B–E).

Contrastingly, most (>75%) oocytes injected with Emi2 siRNA were released from cell cycle arrest, generating fragmented, and 1-, 2-, and 3-cell parthenogenotes in the same time-frame (Figure 4B–D). Fluorescence imaging confirmed the absence of condensed chromosomes aligned on a spindle (Figure 4D, bottom right). Injection of siEmi2, like activation with $SrCl_2$, reduced MBP and H1 phosphorylation compared to siEmi1- and noninjected mII oocytes (Figure 4E). Immunoblotting revealed that mII oocytes injected with siEmi1#2 or siEmi2#1 had respectively reduced levels of Emi1 or Emi2 protein 22 h later (Figure 4F). Since mII is by definition already established in mII oocytes, phenotypes induced by Emi2 siRNAs were not due to interference with this establishment, but with its maintenance.

We sought to show by complementation that phenotypes induced by siEmi2 were due to a reduction in Emi2 protein. Coinjection of siEmi2#1 with baculovirus-expressed Emi2 protein augmented the average proportion of oocytes remaining at mII to 32% compared to a heated control (5%; Figure 4G), representing a modest yet significant ($P<0.001$) rescue. Recombinant Emi2 protein thus displayed an ability to rescue RNAi-mediated depletion of native Emi2.

Injection of mII oocytes with siRNA against Mos mRNA reduced the level of Mos protein 10 h later (Figure 4F). However, Mos mRNA (Supplementary Figure S3) and protein (Figure 4F) were undetectable in noninjected oocytes after ~24 h (~36 h post-hCG), even though aging was not accompanied by a large decrease in the overall protein content (average decrease = 21%, $n = 3$; note also α-tubulin loading controls). Indeed, Mos mRNA had declined after 8 h, to only 17.8% of its level at 4 h (Supplementary Figure S3B). Aged oocytes (at ~36 h post-hCG) retained morphological integrity without signs of cytodegeneration or activation (siEGFP, siMos and siEmi1 panels of Figure 4B and D), with high MBP and H1 kinase activities (Figure 4E). Age-matched oocytes injected with siEGFP or siEmi1 sustained an intact maternal mII spindle (Figure 4D). Oocytes therefore undergo RNAi-independent, autonomous attrition of Mos with age while remaining at mII. The relationship between this attrition and dismantling of the oocyte activation machinery remains to be elucidated.

These data suggest that Emi2 is required to maintain mII arrest in mouse oocytes and is a component of CSF. Release from mII arrest following Emi2 RNAi resulted in cytokinetic dysregulation, with a high incidence of fragmentation (61/174 = 35%) or failure to cleave (51/174 = 29%) 24–30 h after siRNA injection (Figure 4B). In contrast, balanced cleavage occurred for the majority of mII oocytes activated by exposure to the parthenogenetic agent, $SrCl_2$ (109/113 = 96%) or following injection with a sperm-derived oocyte activating extract (SE) containing the physiological SOAF, PLCζ (44/51 = 86%) (Figure 4B) (Fujimoto *et al*, 2004). Cleavage in these cases efficiently produced 2-cell haploid embryos (Figure 4B) capable of subsequent division, arguing against an obligate, dominant haploid-dependent SAC during the first cell cycle (Verlhac *et al*, 1996). No cytodegeneration (0/46) was observed in oocytes exposed to Sr^{2+} ~25 h post-hCG.

These data thus indicate that release from metaphase arrest *per se* (by Emi2 ablation) does not ensure the integrity of the first mitotic cleavage. We infer that in addition to the Emi2-containing pathway that eliminates MPF at fertilization, one or more distinct pathways, possibly also requiring Emi2 and/or Ca_i^{2+}, regulate the second meiotic and possibly first mitotic cytokineses. A role for Emi2 in ensuring productive cytokinesis might explain why some Emi2 persists after activation (Figure 1G and H). To investigate this, we injected mII oocytes with cRNA encoding an Emi2$^{S275N/S279N}$-mCherry fusion, whose Emi2 component contained an S275N/S279N ($DSGX_2S$) phospho-degron mutation. This mutation was predicted to render Emi2 refractory to SCF$^{\beta TrCP}$-potentiated degradation and therefore to be more stable (Margottin-Goguet *et al*, 2003). At 10 h after injection, levels of cRNA were comparable in all samples (data not shown). At this time, oocytes were exposed to the parthenogenetic activating agent, Sr^{2+} and examined 9–10 h later. All oocytes receiving mCherry control cRNA exhibited strong mCherry epifluorescence and had undergone pronuclear activation (Figure 4H). Oocytes injected with Emi2$^{S275N/S279N}$-mCherry-encoding cRNA fell into two classes. Most (72.7%) exhibited

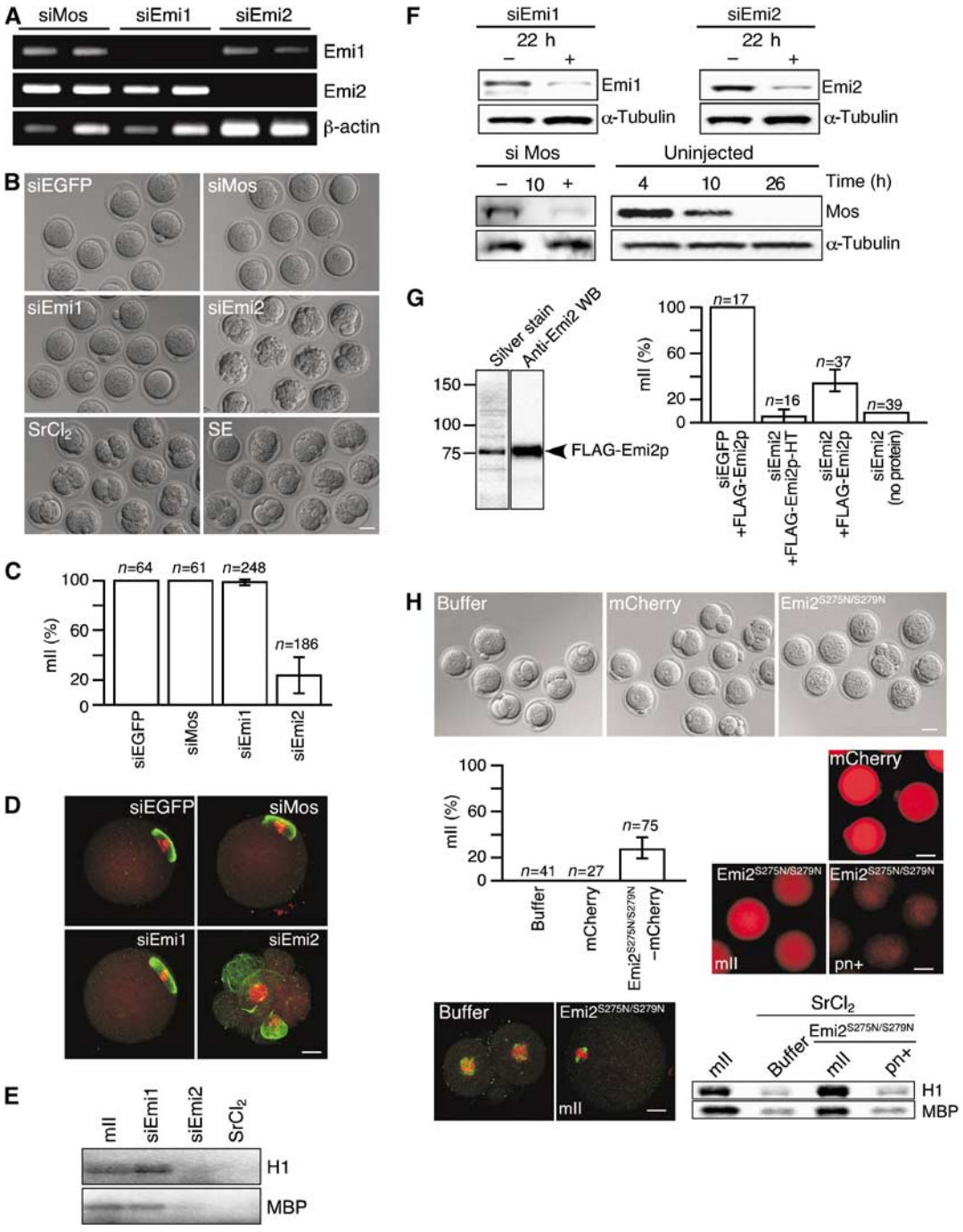

Figure 4 Emi2 mediates mII arrest. (**A**) RT–PCR for Emi1, Emi2 and β-actin transcripts and (**B**) Hoffman modulation microscopy, 23 h after injection of mII oocytes with EGFP, Mos, Emi1 or Emi2 siRNAs, also showing embryos 23 h after activation by exposure of mII oocytes to $SrCl_2$ or injection with sperm-borne oocyte activating extract (SE). Bar = 50 μm. (**C**) Average percentages (showing ranges) of oocytes at mII 23 h after siRNA injection. (**D**) Immunofluorescence microscopy of representative cells in (**B**) showing α-tubulin (green) and genomic DNA (red). Bar = 20 μm. (**E**) Autoradiographic read-out of MBP and H1 kinase assays 22 h after injection of mII oocytes with siEmi1#2 or siEmi2#1, activation with $SrCl_2$ or age-matched mII oocytes that had not been treated (mII). (**F**) Immunoblotting of mII oocytes after injection with siRNA (+) and of aged-matched, uninjected (−) controls for Emi1 and Emi2, 22 h after injection and for Mos 10 h after injection or without injection, showing the autonomous decrease of Mos in uninjected mII oocytes. (**G**) Physical (left) and functional (right) analysis of baculovirus-expressed Emi2-FLAG. Arrest at mII is recorded 23 h after co-injection of siRNA with 5–15 pl freshly-prepared recombinant Emi2 protein (0.3–0.9 mg/ml) as indicated. HT, heated at 70°C for 30 min. (**H**) mII oocytes injected with cRNA encoding mCherry (0.15 μg/μl) or $Emi2^{S275N/S279N}$-mCherry (0.3 μg/μl) followed 10 h later by exposure to $SrCl_2$ and examination 9–10 h after this, showing Hoffman modulation (top panel; bar = 50 μm) and percentages of oocytes apparently arrested at mII (histogram). mCherry (red) epifluorescence is shown for control embryos (mCherry) and nonpronuclear oocytes (mII) and pronuclear embryos (pn+) following injection with $Emi2^{S275N/S279N}$-mCherry cRNA. Bar = 50 μm. Representative cells were subjected to MBP and H1 kinase assays (bottom right) and α-tubulin (green) and genomic DNA fluorescence microscopy as for (E and D) respectively.

pronuclear activation (pn+ in Figure 4H) and low MBP/H1 kinase activities. Epifluorescence in this group was weak but detectable, suggesting low protein levels presumably reflecting $DSGX_2S$-independent degradation. However, members of the second class (27.3%) lacked pronuclei and all exhibited high epifluorescence. These oocytes contained high MBP and H1 kinase activities, condensed chromatin and a compacted spindle (Figure 4H), collectively consistent with their remaining arrested at mII. A correlation between high $Emi2^{S275N/S279N}$ expression and mII arrest would be expected if levels of active recombinant Emi2 remained sufficiently high in the oocytes to inhibit the APC by sequestering an adaptor such as Cdc20. We investigated this possibility for native, wild-type Emi2.

Emi2 transduces cytostatic activity via Cdc20

Emi2 is relatively conserved in its alignment with a binding domain in the C-terminus of Emi1 for the APC adaptor, Cdc20, although an interaction between Cdc20 and Emi2 has not been shown. Using recombinant proteins expressed *in vitro*, immunoprecipitation of Cdc20 readily co-precipitated Emi2 and *vice versa* (Figure 5A). No interaction was observed with a negative control protein. This demonstrates

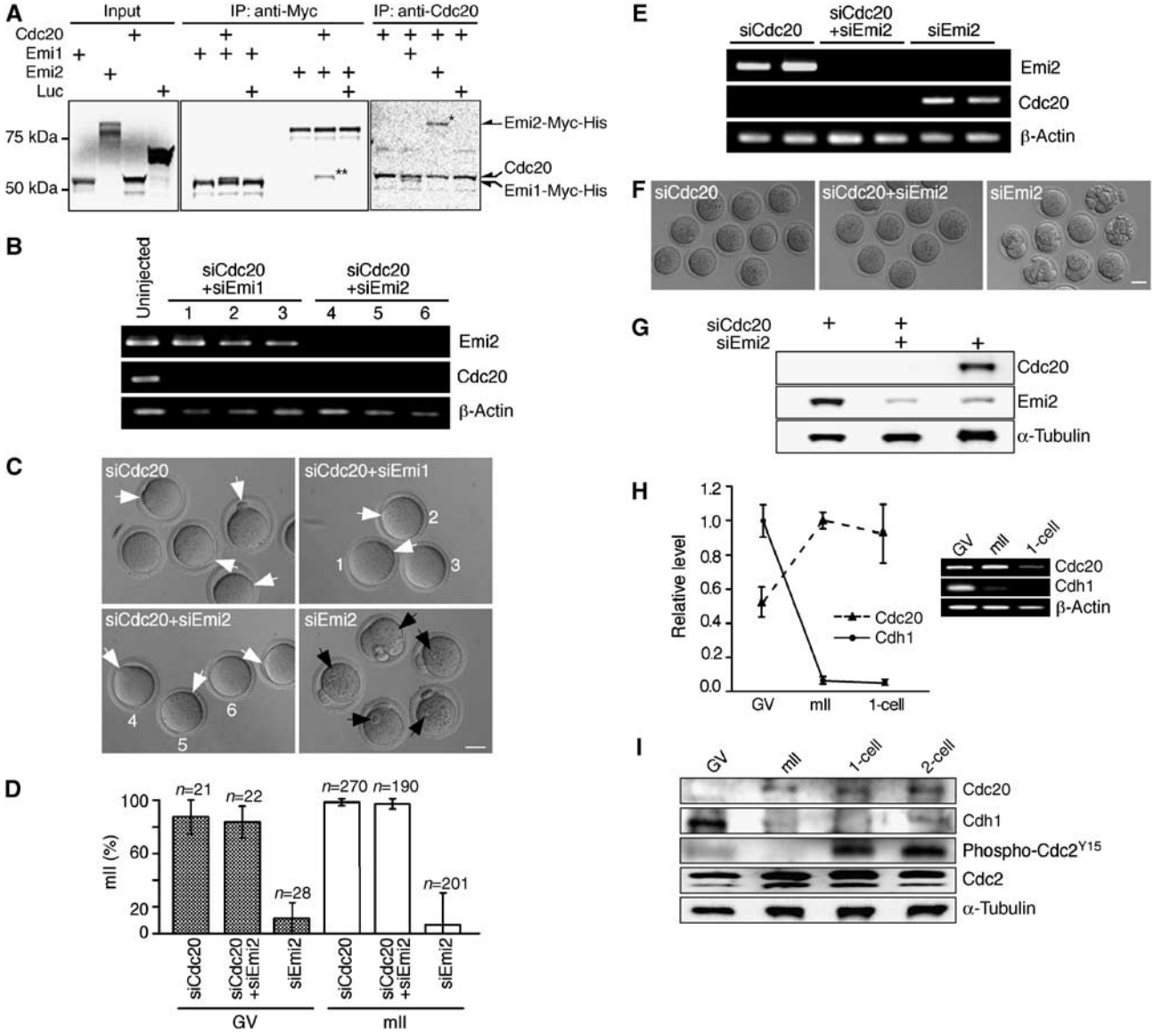

Figure 5 Cytostatic arrest by Emi2 requires Cdc20. (**A**) Co-immunoprecipitation of full-length Cdc20 and Emi1-Myc-His or Emi2-Myc-His fusions produced *in vitro*. Radiolabeled proteins were immunoprecipitated with anti-Cdc20 or anti-Myc antibodies and subjected to SDS–PAGE prior to autoradiography. Co-precipitated proteins corresponding to Emi2-Myc-His and Cdc20 are respectively marked with one or two asterisks. (**B**) RT–PCR for Emi2, Cdc20 and β-actin transcripts 29 h after injection of GV oocytes with [siEmi2#1 + siCdc20#1], [siEmi1#2 + siCdc20#1], siCdc20#1 or without injection. (**C**) Hoffman modulation micrographs of oocytes 29 h after GV oocyte injection as per (B). Numbers in (B) and (C) refer to the same cells; key to labeling is as per Figure 3. Bar = 50 μm. (**D**) Average percentages arrested at mII, respectively, 29 and 23 h after injection of GV (stipled) or mII (open) oocytes with siRNAs as indicated. (**E**) RT–PCR for Emi2, Cdc20 and β-actin transcripts 23 h after injection of mII oocytes with siEmi2#1, [siEmi2#1 + siCdc20#1], or siCdc20#1. (**F**) Phase contrast micrographs 23 h after oocyte injection as per (E). Bar = 50 μm. (**G**) Immunoblotting of mII oocytes 23 h after injection with siRNAs (+) against Cdc20 and/or Emi2 mRNAs. Developmental profiles of (**H**) Cdh1 and Cdc20 mRNA levels shown by (q)PCR (left) and gel electrophoresis, and (**I**) Cdh1, Cdc20, Cdc2 and phospho-$Cdc2^{Y15}$ and α-tubulin (loading control) proteins in a single Western blot.

the stable and discriminatory association of Cdc20 and Emi2 proteins *in vitro*.

To probe the functional relationship between Cdc20 and Emi2, we injected GV oocytes with siEmi2#1 or siCdc20#1 separately or in combination and monitored the reduction of their target transcript levels (Figure 5B). Whereas injection of Emi2 siRNA induced progression through mII, meiotic arrest occurred in maturing oocytes simultaneously injected with Emi2 and Cdc20 siRNAs (Figure 5C and D). Analogous results were obtained 22 h after coinjection of mII-arrested oocytes: ~100% of those coinjected with Emi2 and Cdc20 siRNAs remained at mII (Figure 5D–F; Supplementary Figure S2B). Immunoblotting revealed the presence of 55kDa Cdc20 in mII oocytes, and confirmed a pronounced RNAi-mediated depletion of Emi2 and Cdc20 proteins, mirroring that of their corresponding transcripts (Figure 5E and G; Supplementary Figure S2B). Since co-depletion of Cdc20 and Emi2 did not induce meiotic exit, the loss of Emi2 protein in these and previous experiments (Figure 4A, C and F) was a consequence of RNAi, not of cell cycle progression. These experiments suggest that Emi2 sustains mII arrest via Cdc20.

Why did Cdc20 depletion fail to prevent meiotic progression in maturing oocytes given the requirement of the APC for the mI to mII transition (Terret *et al*, 2003b)? Maturing mouse oocytes contain the APC activator, Cdh1 (Chang *et al*, 2004). However, we found that although Cdh1 mRNA and protein are abundant in maturing (GV) oocytes they decline sharply by mII (Figure 5H and I). This contrasts with Cdc20, whose protein level is low in GV oocytes, but (with its mRNA) becomes higher at mII. From this, Cdc20 is the sole abundant APC adaptor at mII but not during oocyte maturation. This is consistent with the observation that Cdc20 depletion is sufficient to induce an APC-dependent phenotype in mII, but not GV oocytes. We next investigated the physiological implications of this in the context of fertilization.

Cdc20 removal attenuates sperm-induced oocyte activation and parthenogenesis

The equivalence of functional signaling following sperm-induced oocyte activation (fertilization) and parthenogenesis has not been demonstrated. If Emi2 is an essential component of CSF, abrogation of Cdc20 might interfere with fertilization given that the level of Emi2 decreases on oocyte activation (Figure 1F) and Emi2 and Cdc20 mutually interact to sustain mII arrest (Figure 5).

To test this, we first injected mII oocytes with siCdc20#1 or control, EGFP siRNA and incubated them for 8 h, after which the oocytes were still well within their normal fertilizable lifetime (Marston and Chang, 1964). The level of Cdc20 mRNA in siCdc20-injected oocytes decreased on average 97.6% ($n = 40$; Supplementary Figure S2B; see Figure 6A). Immunoblotting confirmed that this reduction was mirrored by a pronounced reduction in the amount of Cdc20 protein (Figure 6B). Cdc20-depleted oocytes were then subjected to

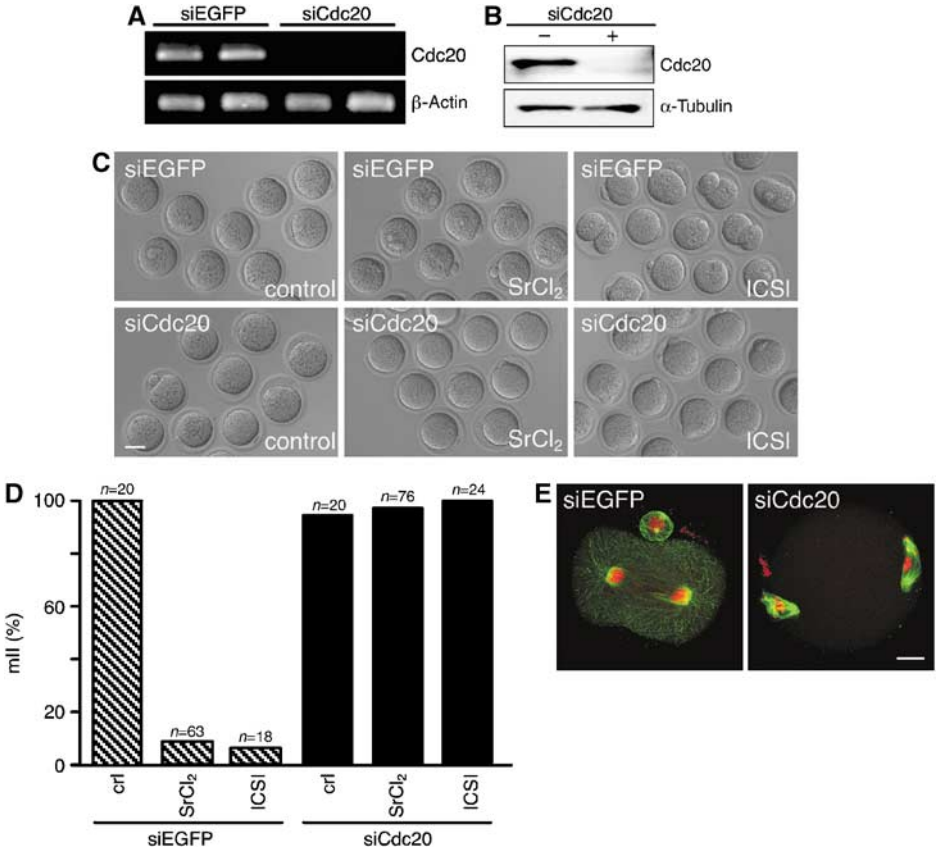

Figure 6 Cdc20 is required for oocyte activation. (**A**) RT–PCR of Cdc20 and β-actin transcripts 8 h after injection of mII oocytes with siEGFP or siCdc20#1 siRNAs. (**B**) Immunoblotting of mII oocytes after injection with Cdc20 siRNA (+) and of aged-matched, uninjected (−) controls. (**C**) Hoffman modulation micrographs and (**D**) percentages remaining at mII of oocytes after injection with siEGFP or siCdc20#1 siRNAs followed 8 h later by exposure to an activation stimulus from either $SrCl_2$ or sperm head injection (ICSI) or no activation stimulus (control) as indicated. Data were recorded 22 h after siRNA injection. Bar = 50 μm. (**E**) Immunofluorescence microscopy of representative cells of (D) following ICSI, showing α-tubulin (green) and DNA in chromatin (red). Bar = 20 μm.

an activation stimulus, either by exposure to $SrCl_2$ or by injection with a sperm head (Perry *et al*, 1999). At 13 h after receiving either of these activating stimuli, all (100%) control oocytes injected with EGFP siRNA possessed pronuclei and/or second Pbs indicative of oocyte activation (Figure 6C and D). Contrastingly, oocytes injected with Cdc20 siRNA prior to $SrCl_2$ exposure or sperm head injection did not become activated (Figure 6C–E). Where sperm had been injected, oocytes possessed two clusters of metaphase chromosomes, corresponding to paternal and maternal chromatin (Figure 6E, right panel). Thus, Cdc20 is essential for the induction of cell cycle progression by spermatozoa or in $SrCl_2$-induced parthenogenesis. This argues against redundant or alternative signaling mechanisms downstream of Emi2 in fertilization and provides direct evidence that activation pathways in fertilization and parthenogenesis operate through a common node that requires Cdc20.

Discussion

This study addresses the molecular nature of CSF in intact mouse mII oocytes. Once metaphase is established, CSF activity requires Emi2. The abrogation of Emi2-mediated mII arrest in $SrCl_2$- or sperm-induced oocyte activation is transduced via Cdc20. High levels of Emi2 in the testis (Figure 1F) suggest that it plays a role in male meiosis.

Work in *Xenopus* recently suggested that the putative Emi2 ortholog, XErp1/Emi2, has CSF activity (Liu and Maller, 2005; Rauh *et al*, 2005; Schmidt *et al*, 2005; Tung *et al*, 2005). These studies do not exclude a cytostatic role for Emi1 independently of Emi2 at mII. However, we detected only a low level of 48 kDa Emi1 in mouse mII oocytes, and the level increases at least 1.2-fold in the first two mitotic cell cycles and remains detectable throughout preimplantation development (Figure 1F). Notwithstanding this, a truncated form of Emi1 in mouse oocytes has been reported to contribute to mII arrest (Paronetto *et al*, 2004). That report conceptually addressed meiotic metaphase arrest but focused on the behavior of recombinant protein in mitotic cells and their extracts. The specificity of anti-Emi1 antibodies was not shown with respect to Emi2. This might have been circumvented by the introduction into GV oocytes of a long (447 nucleotide) dsRNA mapping to the 3′ end of Emi1, but depletion of Emi1 mRNA was not shown quantitatively nor the effects of injection clearly documented (see Figure 8B of Paronetto *et al*, 2004). Long dsRNAs are more likely to lack the specificity of siRNAs (Haley and Zamore, 2004) and the dsRNA segment employed (corresponding to the C-terminus of Emi1) is conserved with respect to Emi2 (Figure 1A); any effect of Emi1 dsRNA injection on levels of Emi2 mRNA and protein was not reported. Finally, the study reports a functional cytostatic interaction between Emi1 and Rsk, yet oocytes from triple *Rsk* (*1*, *2* and *3*) *null* mice exhibit CSF arrest (Dumont *et al*, 2005).

Work presented here dissects CSF arrest *in situ*, in intact mouse oocytes and embryos using an siRNA-mediated RNAi-based approach (Elbashir *et al*, 2001; Hannon and Rossi, 2004). Transcriptomic analysis indicated 'off-target' RNAi by siRNAs only when at least 11 contiguous nucleotides were shared between the siRNA and its non-intended target (Jackson *et al*, 2003). We took this into consideration and followed recent recommendations to achieve siRNA target specificity (Huppi *et al*, 2005). By eliciting the reduction of target proteins *in situ*, RNAi obviates the need to infer function from ectopic expression or exogenous introduction of protein or antibodies with limited knowledge of their specific activity, specificity or appropriate level, modification or localization.

This approach revealed that in addition to being a major component of CSF, Emi2 may be a cytoskeletal regulator in that its removal in both maturing and mII oocytes resulted in aberrant cleavage behaviour (Figures 3B and 4B; Supplementary movie S1). This frequently manifested itself as fragmentation, which putatively reflects a lack of coordination between microtubule and microfilament dynamics at the time of cytokinesis following mouse oocyte activation (Alikani *et al*, 2005). An alternative explanation is that aberrant cytokinesis reflected the time taken for Emi2 siRNA to induce metaphase release; cytodegeneration could be a function of oocyte age. This is unlikely, because exposure of oocytes to Sr^{2+} 24–25 h post-hCG corresponds to the time at which siEmi2-induced meiotic exit becomes apparent (unpublished observations), although Sr^{2+}-activation of such age-matched oocytes produces normal second Pb extrusion and pronuclear formation without fragmentation (Figure 6C).

Germane to the function of Emi2 in cytokinesis is its fate after oocyte activation. Emi2 declined to at least 18% of its mII level following fertilization (Figure 1G) and more gradually after parthenogenetic activation (Figure 1H). Expression of a stable form of Emi2 followed by Sr^{2+} exposure 10 h later elicited mII arrest when expression levels were apparently high (Figure 4H). Even where epifluorescence was relatively weak, it was stronger than that produced by an Emi2-mCherry control, in which it was undetectable (data not shown). Together, these findings suggest that while the S275N/S279N mutation confers some stability, Emi2 degradation in mII oocytes is not entirely regulated via the $DSGX_2S$ phospho-degron. This might explain why some Emi2 protein persists after meiotic exit, perhaps to coordinate cytokinesis either directly or otherwise. It remains to be seen whether discrete populations of Emi2 with different functions are regulated by different degradation pathways.

Although not required for CSF arrest in the mouse, the SAC is clearly coordinated with cortical microfilament dynamics and meiotic exit; disruption of Emi2 absent other oocyte activation signals represents a situation in which this coordination does not occur. These pathways may be differently linked in *Xenopus* oocytes, which—unlike those of the mouse—are sensitive to mechanical activation (Charbonneau and Grey, 1984). Signaling and cytoskeletal changes might be linked in mammals by MISS (Lefebvre *et al*, 2002), DOC1R (Terret *et al*, 2003a), Plk1 (discussed below) or other molecules affecting microtubule dynamics.

Cdc20 is required to transduce sperm- or $SrCl_2$-induced activating stimuli. This suggests that parthenogenesis and fertilization operate via convergent or identical pathways and that sperm lack Cdc20-independent redundancy in the signaling by which they induce meiotic progression. This is not axiomatic; the APC^{cdh1} complex may play a meiotic role (Chang *et al*, 2004), the E3 ubiquitin ligase RFLP4 is present in mouse oocytes (Suzumori *et al*, 2003), and Cdc20-independent inhibition of the APC in *Xenopus* oocytes has been reported for the ubiquitin ligase, Xnf7 (Casaletto *et al*, 2005).

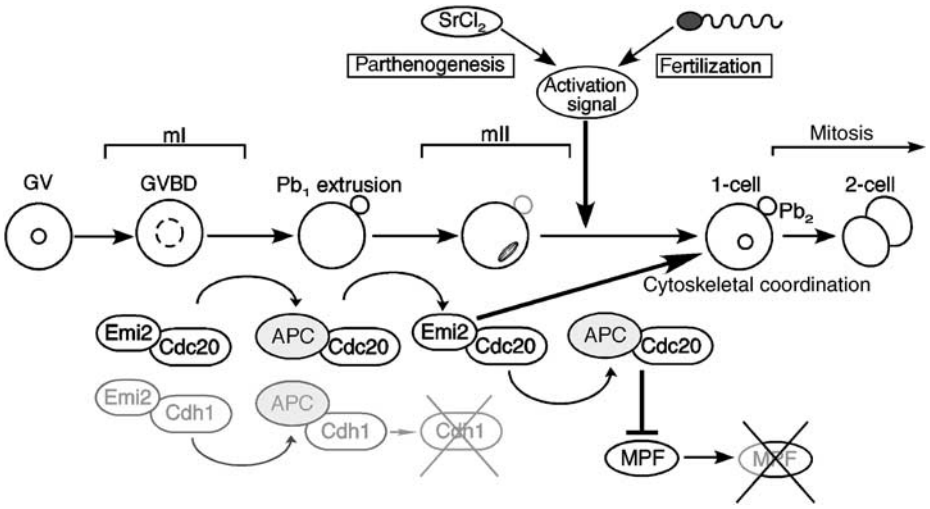

Figure 7 Emi2-Cdc20 in mammalian meiosis and meiotic exit. In this model, suspension of meiosis at mII occurs because Emi2 sequesters Cdc20. This suspension is resolved by an activating stimulus—induced by sperm or parthenogenetic agent such as $SrCl_2$, for example—that signals to release Cdc20 from $Emi2^{Cdc20}$, enabling the generation of active APC^{Cdc20}. The APC adaptor Cdh1 is implicated in mI, but Cdh1 is inactivated or destroyed by mII. Thus, Cdc20 apparently functions as an obligate signal transduction node connecting the oocyte activating stimulus to meiotic exit. A subpopulation of Emi2 remains following activation to ensure productive cytokinesis. Pb_1 and Pb_2 are first and second polar bodies, respectively.

The interaction with Cdc20 is apparently a cardinal feature of Emi2 CSF activity in oocytes, consistent with a model in which Emi2 sequesters Cdc20 to inhibit the APC until the interaction is relieved during oocyte activation (Figure 7). Both sperm and Sr^{2+} stimulate Ca_i^{2+} oscillations as a prelude to mammalian (but not amphibian) oocyte activation (Runft *et al*, 2002), and such oscillations are synchronized with the oscillatory activity of CaMKII (Markoulaki *et al*, 2003). Moreover, constitutively active CaMKII induces Ca_i^{2+}-independent meiotic progression *Xenopus* (Lorca *et al*, 1993). *Xenopus* Emi2 is targeted for destruction by Plx1 phosphorylation in a manner that is potentiated by CaMKII phosphorylation (Liu and Maller, 2005; Rauh *et al*, 2005; Schmidt *et al*, 2005). By analogy to *Xenopus*, dual phosphorylation targets mammalian Emi2 for βTrCP-mediated degradation in response to sperm-induced $[Ca_i^{2+}]$ elevation, although some Emi2 persists following activation (Figure 1G and H; discussed above). Notably, the mammalian ortholog of Plx1, Plk1, also regulates microtubule assembly during mouse oocyte maturation and fertilization (Tong *et al*, 2002). Given that Plk1 is inhibited by DNA-responsive check-points in mitotic mammalian cells (Smits *et al*, 2000), its association with Emi2 plausibly coordinates cell cycle modulation, cytokinesis and paternal genome sensing at fertilization (Perry, 2000; Tong *et al*, 2002; Stokes and Michael, 2003).

The clear implication of this work is that Emi2 is an essential component of mammalian CSF. A molecular dissection of Emi2 will shed light on the conditions that must be satisfied at fertilization for full development. In particular, the employment of RNAi in intact cells promises to illuminate the relationship between Emi2, cell cycle resumption and cytokinesis.

Materials and methods

Gamete preparation and culture of oocytes and embryos

Germinal vesicle (GV) oocyte collection from ovaries of 8- to 12-week-old $B6D2F_1$ female mice, primed with eCG 46–48 h previously, were placed in M2 medium (Sigma) supplemented with 150 μM isobutylmethylxanthine (M2-IBMX) (Kim *et al*, 2002). Cumulus-denuded oocytes were washed and cultured in M2-IBMX. After injection, oocytes were washed and cultured in M2 medium lacking IBMX. $B6D2F_1$ mII oocytes were collected in CZB-H at least 12 h after hCG injection and cultured in CZB (Fujimoto *et al*, 2004). Parthenogenetic activation was by exposure to 5 mM $SrCl_2$ in Ca^{2+}-free CZB for 1–4 h or by injection of a sperm-borne oocyte activating extract (SE) (Fujimoto *et al*, 2004). Nascent haploid embryos were washed thoroughly in CZB lacking the activating agent and incubation continued. All culture was under mineral oil (Shire, Florence, KT) in humidified, 5% (v/v) CO_2/air at 37°C. Preparation of developmentally competent, membrane-challenged spermatozoa was as described previously (Perry *et al*, 1999; Fujimoto *et al*, 2004).

Microinjection of protein

Microinjection was with a piezo-actuated pipette (Prime Tech, Japan). Parthenogenetically activated $B6D2F_1$ haploid zygotes (6 h after first $SrCl_2$ exposure) or 2-cell embryos (22–25 h after first $SrCl_2$ exposure) were injected with mII (17–22 h post-hCG) ooplasm within 10 min of its removal. We estimate that 15 to >25 pl was introduced per injection (needle tip diameter = 5–6 μm). In some experiments, mII ooplasm was from a genetically marked (transgenic) donor strain expressing mitochondrially targeted Venus protein (Okita *et al*, 2004), allowing verification of cytoplasmic transfer by RT–PCR or fluorescence microscopy. ~5 pl per oocyte of freshly purified baculovirus-expressed recombinant Emi2 was injected in 5% (w/v) PVP (M_r 360 000) at 0.3–0.9 mg/ml. Where appropriate, recombinant Emi2 was heated to 70°C for 30 min. Data were analyzed with the χ^2 test.

RNA injection

For siRNA injection, GV oocytes were placed in M2 medium, microinjected through a borosilicate glass pipette (tip diameter, <1 μm) with siRNA (25 μM in phosphate-buffered saline) and washed and cultured in M2 for a further 25–50 h prior to analysis. mII oocytes were injected typically 13.5–14.5 h post-hCG administration, with siRNA (25 μM in a solution containing 9–15% (w/v) PVP_{360}) or cRNA (0.15–0.3 μg/μl in 7% (w/v) PVP_{360}) through a tip of diameter 5 μm and washed and cultured in CZB or KSOM for a further 20–31 h prior to analysis; 23 h post-injection corresponds to 35 h post-hCG. Injections were completed within 1 h of sample/PVP mixing. Where appropriate, 8–10 h after siRNA or cRNA injection oocytes were activated by exposure to $SrCl_2$ (5mM in Ca^{2+}-free CZB) for 1–3 h or by intracytoplasmic sperm injection (ICSI) and

cultured in CZB or KSOM. Data are from at least two replicates per experiment.

Supplementary data

Supplementary data are available at *The EMBO Journal* Online.

Acknowledgements

We are grateful to Dr Timm Schroeder for the mito-Venus construct, to the Tsien lab for mCherry plasmid DNA and for grant support from the RIKEN President's Fund and a Grant-in-Aid (No. 80360486) from the Japan Society for the Promotion of Science.

References

Alikani M, Schimel T, Willadsen SM (2005) Cytoplasmic fragmentation in activated eggs occurs in the cytokinetic phase of the cell cycle, in lieu of normal cytokinesis, and in response to cytoskeletal disorder. *Mol Hum Reprod* **11:** 335–344

Casaletto JB, Nutt LK, Wu Q, Moore JD, Etkin LD, Jackson PK, Hunt T, Kornbluth S (2005) Inhibition of the anaphase-promoting complex by the Xnf7 ubiquitin ligase. *J Cell Biol* **169:** 61–71

Chang HY, Levasseur M, Jones KT (2004) Degradation of APCcdc20 and APCcdh1 substrates during the second meiotic division in mouse eggs. *J Cell Sci* **117:** 6289–6296

Charbonneau M, Grey RD (1984) The onset of activation responsiveness during maturation coincides with the formation of the cortical endoplasmic reticulum in oocytes of *Xenopus laevis*. *Dev Biol* **102:** 90–97

Choi T, Fukasawa K, Zhou R, Tessarollo L, Borror K, Resau J, Vande Woude GF (1996) The Mos/mitogen-activated protein kinase (MAPK) pathway regulates the size and degradation of the first polar body in maturing mouse oocytes. *Proc Natl Acad Sci USA* **93:** 7032–7035

Colledge WH, Carlton MB, Udy GB, Evans MJ (1994) Disruption of c-mos causes parthenogenetic development of unfertilized mouse eggs. *Nature* **370:** 65–68

Dumont J, Umbhauer M, Rassinier P, Hanauer A, Verlhac MH (2005) p90Rsk is not involved in cytostatic factor arrest in mouse oocytes. *J Cell Biol* **169:** 227–231

Elbashir SM, Harborth J, Lendeckel W, Yalcin A, Weber K, Tuschl T (2001) Duplexes of 21-nucleotide RNAs mediate RNA interference in cultured mammalian cells. *Nature* **411:** 494–498

Fang G, Yu H, Kirschner MW (1998) The checkpoint protein MAD2 and the mitotic regulator CDC20 form a ternary complex with the anaphase-promoting complex to control anaphase initiation. *Genes Dev* **12:** 1871–1883

Fujimoto S, Yoshida N, Fukui T, Amanai M, Isobe T, Itagaki C, Izumi T, Perry ACF (2004) Mammalian phospholipase Cζ induces oocyte activation from the sperm perinuclear matrix. *Dev Biol* **274:** 370–383

Gross SD, Schwab MS, Lewellyn AL, Maller JL (1999) Induction of metaphase arrest in cleaving *Xenopus* embryos by the protein kinase p90Rsk. *Science* **286:** 1365–1367

Haccard O, Sarcevic B, Lewellyn A, Hartley R, Roy L, Izumi T, Erikson E, Maller JL (1993) Induction of metaphase arrest in cleaving *Xenopus* embryos by MAP kinase. *Science* **262:** 1262–1265

Haley B, Zamore PD (2004) Kinetic analysis of the RNAi enzyme complex. *Nat Struct Mol Biol* **11:** 599–606

Hannon GJ, Rossi JJ (2004) Unlocking the potential of the human genome with RNA interference. *Nature* **431:** 371–378

Hashimoto N, Watanabe N, Furuta Y, Tamemoto H, Sagata N, Yokoyama M, Okazaki K, Nagayoshi M, Takeda N, Ikawa Y, Aizawa S (1994) Parthenogenetic activation of oocytes in c-mos-deficient mice. *Nature* **370:** 68–71

Huppi K, Martin SE, Caplen NJ (2005) Defining and assaying RNAi in mammalian cells. *Mol Cell* **17:** 1–10

Jackson AL, Bartz SR, Schelter J, Kobayashi SV, Burchard J, Mao M, Li B, Cavet G, Linsley PS (2003) Expression profiling reveals off-target gene regulation by RNAi. *Nat Biotechnol* **21:** 635–637

Kim MH, Yuan X, Okumura S, Ishikawa F (2002) Successful inactivation of endogenous Oct-3/4 and c-mos genes in mouse preimplantation embryos and oocytes using short interfering RNAs. *Biochem Biophys Res Comm* **296:** 1372–1377

Kline D, Kline JJ (1992) Repetitive calcium transients and the role of calcium in exocytosis and cell cycle activation in the mouse egg. *Dev Biol* **149:** 80–89

Lefebvre C, Terret ME, Djiane A, Rassinier P, Maro B, Verlhac MH (2002) Meiotic spindle stability depends on MAPK-interacting and spindle-stabilizing protein (MISS), a new MAPK substrate. *J Cell Biol* **157:** 603–613

Li Y, Gorbea C, Mahaffey D, Rechsteiner M, Benezra R (1997) MAD2 associates with the cyclosome/anaphase-promoting complex and inhibits its activity. *Proc Natl Acad Sci USA* **94:** 12431–12436

Liu J, Maller JL (2005) Calcium elevation at fertilization coordinates phosphorylation of XErp1/Emi2 by Plx1 and CaMK II to release metaphase arrest by cytostatic factor. *Curr Biol* **15:** 1–11

Lorca T, Cruzalegui FH, Fesquet D, Cavadore JC, Mery J, Means A, Doree M (1993) Calmodulin-dependent protein kinase II mediates inactivation of MPF and CSF upon fertilization of *Xenopus* eggs. *Nature* **366:** 270–273

Margottin-Goguet F, Hsu JY, Loktev A, Hsieh HM, Reimann JD, Jackson PK (2003) Prophase destruction of Emi1 by the SCF(betaTrCP/Slimb) ubiquitin ligase activates the anaphase promoting complex to allow progression beyond prometaphase. *Dev Cell* **4:** 813–826

Markoulaki S, Matson S, Ducibella T (2003) Fertilization stimulates long-lasting oscillations of CaMKII activity in mouse eggs. *Dev Biol* **272:** 15–25

Marston JH, Chang MC (1964) The fertilizable life of ova and their morphology following delayed insemination in mature and immature mice. *J Exp Zool* **155:** 237–251

Masui Y (2000) The elusive cytostatic factor in the animal egg. *Nat Rev Mol Cell Biol* **1:** 228–232

Masui Y, Markert CL (1971) Cytoplasmic control of nuclear behavior during meiotic maturation of frog oocytes. *J Exp Zool* **177:** 129–145

Murray AW, Solomon MJ, Kirschner MW (1989) The role of cyclin synthesis and degradation in the control of maturation promoting factor activity. *Nature* **339:** 280–286

Ohsumi K, Koyanagi A, Yamamoto TM, Gotoh T, Kishimoto T (2004) Emi1-mediated M-phase arrest in *Xenopus* eggs is distinct from cytostatic factor arrest. *Proc Natl Acad Sci USA* **101:** 12531–12536

Okita C, Sato M, Schroeder T (2004) Generation of optimized yellow and red fluorescent proteins with distinct subcellular localization. *Biotechniques* **36:** 418–422

Page AM, Hieter P (1999) The anaphase-promoting complex: new subunits and regulators. *Ann Rev Biochem* **68:** 583–609

Paronetto MP, Giorda E, Carsetti R, Rossi P, Geremia R, Sette C (2004) Functional interaction between p90Rsk2 and Emi1 contributes to the metaphase arrest of mouse oocytes. *EMBO J* **23:** 4649–4659

Perry ACF (2000) Hijacking oocyte DNA repair machinery in transgenesis? *Mol Reprod Dev* **56:** 319–324

Perry ACF, Wakayama T, Yanagimachi R (1999) A novel trans-complementation assay suggests full mammalian oocyte activation is coordinately initiated by multiple, submembrane sperm components. *Biol Reprod* **60:** 747–755

Pikó L, Taylor KD (1987) Amounts of mitochondrial DNA and abundance of some mitochondrial gene transcripts in early mouse embryos. *Dev Biol* **123:** 364–374

Rauh NR, Schmidt A, Bormann J, Nigg EA, Mayer TU (2005) Calcium triggers exit from meiosis II by targeting the APC/C inhibitor XErp1 for degradation. *Nature* **437:** 1048–1052

Reimann JD, Freed E, Hsu JY, Kramer ER, Peters JM, Jackson PK (2001) Emi1 is a mitotic regulator that interacts with Cdc20 and inhibits the anaphase promoting complex. *Cell* **105:** 645–655

Reimann JD, Jackson PK (2002) Emi1 is required for cytostatic factor arrest in vertebrate eggs. *Nature* **416:** 850–854

Runft LL, Jaffe LA, Mehlmann LM (2002) Egg activation at fertilization: where it all begins. *Dev Biol* **245:** 237–254

Sagata N, Watanabe N, Vande Woude GF, Ikawa Y (1989) The c-mos proto-oncogene product is a cytostatic factor responsible for meiotic arrest in vertebrate eggs. *Nature* **342:** 512–518

Saunders CM, Larman MG, Parrington J, Cox LJ, Royse J, Blayney LM, Swann K, Lai FA (2002) PLCζ: a sperm-specific trigger of Ca^{2+} oscillations in eggs and embryo development. *Development* **129:** 3533–3544

Schmidt A, Duncan PI, Rauh NR, Sauer G, Fry AM, Nigg EA, Mayer TU (2005) *Xenopus* polo-like kinase Plx1 regulates XErp1, a novel inhibitor of APC/C activity. *Genes Dev* **19:** 502–513

Smits VA, Klompmaker R, Arnaud L, Rijksen G, Nigg EA, Medema RH (2000) Polo-like kinase-1 is a target of the DNA damage checkpoint. *Nat Cell Biol* **2:** 672–676

Stokes MP, Michael WM (2003) DNA damage-induced replication arrest in *Xenopus* egg extracts. *J Cell Biol* **163:** 245–255

Suzumori N, Burns KH, Yan W, Matzuk MM (2003) RFPL4 interacts with oocyte proteins of the ubiquitin-proteasome degradation pathway. *Proc Natl Acad Sci USA* **100:** 550–555

Svoboda P, Stein P, Hayashi H, Schultz RM (2000) Selective reduction of dormant maternal mRNAs in mouse oocytes by RNA interference. *Development* **127:** 4147–4156

Tang Z, Bharadwaj R, Li B, Yu H (2001) Mad2-Independent inhibition of APCCdc20 by the mitotic checkpoint protein BubR1. *Dev Cell* **1:** 227–237

Terret ME, Lefebvre C, Djiane A, Rassinier P, Moreau J, Maro B, Verlhac MH (2003a) DOC1R: a MAP kinase substrate that control microtubule organization of metaphase II mouse oocytes. *Development* **130:** 5169–5177

Terret ME, Wassmann K, Waizenegger I, Maro B, Peters JM, Verlhac MH (2003b) The meiosis I-to-meiosis II transition in mouse oocytes requires separase activity. *Curr Biol* **13:** 1797–1802

Tong C, Fan HY, Lian L, Li SW, Chen DY, Schatten H, Sun QY (2002) Polo-like kinase-1 is a pivotal regulator of microtubule assembly during mouse oocyte meiotic maturation, fertilization, and early embryonic mitosis. *Biol Reprod* **67:** 546–554

Tsurumi C, Hoffmann S, Geley S, Graeser R, Polanski Z (2004) The spindle assembly checkpoint is not essential for CSF arrest of mouse oocytes. *J Cell Biol* **167:** 1037–1050

Tung JJ, Hansen DV, Ban KH, Loktev AV, Summers MK, Adler III JR, Jackson PK (2005) A role for the anaphase-promoting complex inhibitor Emi2/XErp1, a homolog of early mitotic inhibitor 1, in cytostatic factor arrest of Xenopus eggs. *Proc Natl Acad Sci USA* **102:** 4318–4323

Tunquist BJ, Eyers PA, Chen LG, Lewellyn AL, Maller JL (2003) Spindle checkpoint proteins Mad1 and Mad2 are required for cytostatic factor-mediated metaphase arrest. *J Cell Biol* **163:** 1231–1242

Tunquist BJ, Schwab MS, Chen LG, Maller JL (2002) The spindle checkpoint kinase bub1 and cyclin e/cdk2 both contribute to the establishment of meiotic metaphase arrest by cytostatic factor. *Curr Biol* **12:** 1027–1033

Verlhac MH, Kubiak JZ, Weber M, Geraud G, Colledge WH, Evans MJ, Maro B (1996) Mos is required for MAP kinase activation and is involved in microtubule organization during meiotic maturation in the mouse. *Development* **122:** 815–822

Watanabe N, Hunt T, Ikawa Y, Sagata N (1991) Independent inactivation of MPF and cytostatic factor (Mos) upon fertilization of *Xenopus* eggs. *Nature* **352:** 247–248

Wianny F, Zernicka-Goetz M (2000) Specific interference with gene function by double-stranded RNA in early mouse development. *Nat Cell Biol* **2:** 70–75

Yu H, Peters JM, King RW, Page AM, Hieter P, Kirschner MW (1998) Identification of a cullin homology region in a subunit of the anaphase-promoting complex. *Science* **279:** 1219–1222

Zernicka-Goetz M, Ciemerych MA, Kubiak JZ, Tarkowski AK, Maro B (1995) Cytostatic factor inactivation is induced by a calcium-dependent mechanism present until the second cell cycle in fertilized but not in parthenogenetically activated mouse eggs. *J Cell Sci* **108:** 469–474